Development and Validation of Bolted Connection Modeling in LS-DYNA® for Large Vehicle Models

Michalis Hadjioannou, David Stevens, Matt Barsotti
Protection Engineering Consultants LLC, Austin, TX, USA

Abstract

As part of the United States Marine Corps (USMC) Mitigation of Blast Injuries through Modeling and Simulation project, Protection Engineering Consultants performed numerical and experimental investigations to develop modeling approaches for bolted connections. Vehicle models require efficient yet accurate methods to represent bolted connections, especially under extreme loading situations where connection behavior may have crucial impact on the accurate prediction of the response. Efficient connection models require relatively coarse mesh sizes and computationally cheap element types that allow modeling large numbers of connections in vehicle models. This paper describes the development and validation of reduced bolted connection models that utilize a combination of beam and shell elements. The models were developed and validated with data from bolted connections that were tested under static and dynamic loading conditions. The tests provided valuable data for the refinement of the models, which are shown capable of simulating connection behavior up to and including rupture.

Important aspects of the modeling procedure are highlighted including contact definitions and bolt preloading, as well as inherent limitations that exist in such models. The study also demonstrates the importance of material failure parameters such as triaxiality-dependent and strain-rate-dependent fracture. These parameters influence not only the connection capacity but also the absorbed energy before the connection fails. Considerations of the absorbed energy are crucial when assessing the safety of occupants in vehicles under extreme loading conditions.

Introduction

As part of the United States Marine Corps (USMC) Mitigation of Blast Injuries through Modeling and Simulation project, a simplified yet accurate methodology was developed to simulate the behavior of steel bolted connections including rupture. This methodology is useful when there is a need to model numerous bolted connections in vehicle models. The design of commercial and military vehicles is an iterative procedure and requires the evaluation of different design options to meet performance criteria. Therefore, such models need to be computationally cheap and easy to construct but they also have to provide accurate results. Accurate representation of bolted connections in vehicle models is crucial especially when the vehicle design focuses on occupant safety using components that are designed to absorb energy under extreme loading conditions, such as collisions, explosions, etc.

Previous efforts in connection modeling provided a basis for the development of the proposed simplified modeling methodology presented in this paper. A number of research studies focused on simplified modeling approaches on bolted connections [1,2]. Depending on the application of the finite element model and the purpose of the analysis, bolts can be represented with merged nodes of separate components at the physical locations of the bolts or can be as detailed as including a finely meshed bolt with the nut tightened by representing the bolt threads.

Between these two extremes, there are other simplified (reduced) approaches that can potentially represent the connection behavior with good accuracy and at the same time have significant gains in terms of computational expense. Sonnenschein [3] has reviewed a number of alternative simplified modeling procedures of bolted connections using LS-DYNA. A commonly used approach utilizes beam elements to simulate the bolt shank; these are attached to beam elements arranged radially around the bolt hole, also known as a spider mesh. The spider mesh is intended to represent the bolt head and nut. This approach eliminates the need of contact definitions which can result in inaccurate representation of the bearing stresses that are developed between the bolt shank and the bolt hole. For that reason, the typical failure modes associated with bolted connections such as plate tear-out rupture and bolt shear failure cannot be captured.

Sonnenschein [3] suggested an intermediate approach which can account for the bearing stresses of the bolt in the bolt-hole by avoiding the need to use solid elements. In this case the bolt head is modelled with shell elements which are connected with beam elements that represent the bolt shank. The bolt shank interacts with the bolt hole through null beam elements that are placed around the hole. An alternative to that approach was proposed by Narkhede *et al* [2] that uses discrete spring elements to account for the interaction of the bolt shank with the bolt hole. These two approaches show good agreement with experimental results but neither was capable of explicitly capturing the connection response up to failure or the failure mode.

The proposed simplified modeling methodology not only captures the connection behavior at the early loading stages, but it is also able to capture connection rupture with good accuracy either under static or dynamic loading conditions. The method was rigorously validated against connections that were physically tested under dynamic and static loading conditions until complete failure. The data gathered from these tests provided a basis for the development and validation of simplified bolted connection models. These models use beam and shells elements to explicitly represent important characteristics of bolted connections such as bolt preloading, interaction of the separate connection components through contact definitions, and physical fracture of the connecting parts. Certain limitations of the modeling procedure were also identified and are discussed in this paper.

Static and Dynamic Pendulum Testing of Bolted Connections

Experiments

Protection Engineering Consultants (PEC) designed a series of tests on bolted connections to provide data for the validation of simplified modeling approaches for bolted connections. The tests applied direct shear to bolted connections as shown in Fig. 1; different bolt diameters, plate thicknesses, and bolt-hole to edge distances were evaluated. By adjusting these parameters, typical failure modes were achieved including plate tear-out failure and direct shear fracture of the bolt as shown in Fig. 2.

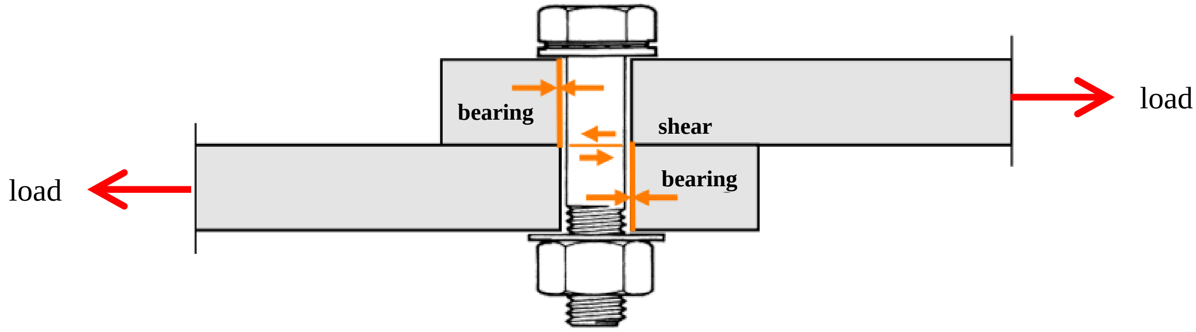

Fig. 1: Bolted connection loaded in direct shear

(a) plate tear-out failure

(b) Bolt shear fracture

Fig. 2: Typical failure modes of physical tests; (a) plate tear-out failure, (b) bolt shear fracture

The tests were performed by Southwest Research Institute (SwRI) using a universal loading machine for the static tests and a 2250-lbf pendulum for the dynamic tests; see Fig. 3. By adjusting the drop-height of the pendulum, different load rates were achieved. The connection specimens were loaded through a specially designed frame that accommodated the connection specimens shown in Fig. 3(b). Similar test specimens to those that were tested dynamically were also tested statically until total failure. A total of twenty-four pendulum and seven static tests were performed during the testing program. All specimens consisted of rolled homogeneous armor (RHA) steel plates and Grade 8 bolts. Similar tests were performed with welded connection specimens but they are outside the scope of this paper. The data gathered from these tests were used to validate the simplified bolted connection models.

The strains in all specimens were measured using digital image correlation (DIC). In particular, for the dynamic tests, the peak axial strain (thus peak axial force), the pendulum impact velocity and failure mode were used as the basis for comparison with the numerical models. In addition, the static tests were instrumented with conventional load cells and string potentiometers since these test configurations allowed their usage.

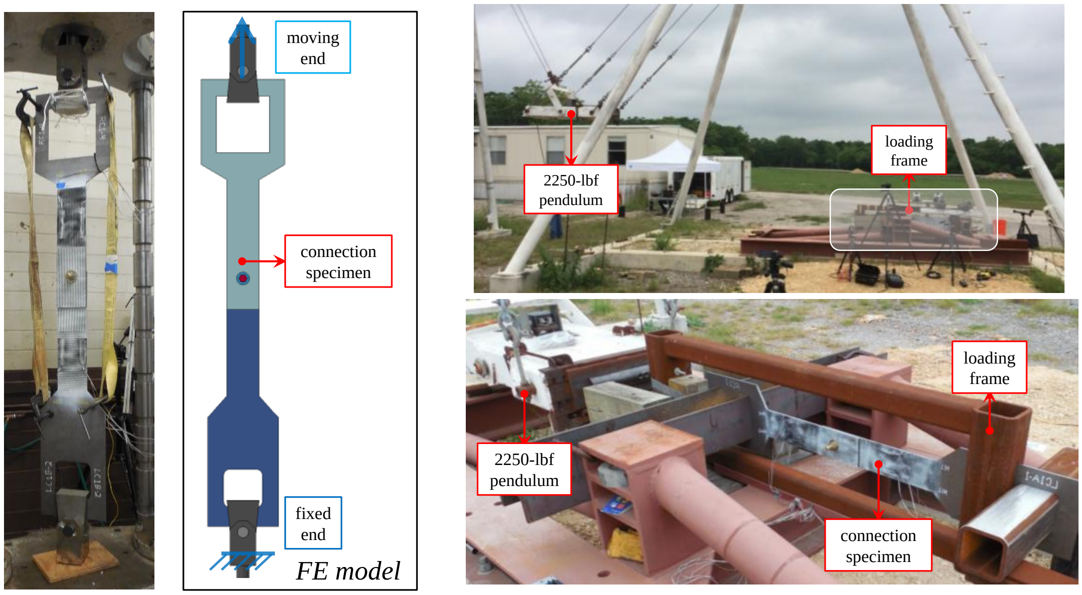

(a) static testing (b) dynamic testing

Fig. 3: Testing apparatus used for the connection tests; (a) static testing, (b) dynamic testing

Proposed Simplified Modeling Procedure

Generating the Finite Element Mesh

The bolt-head and nut are represented with fully integrated shell elements (elform=16) that are placed in the surface defined from the bolt-head and nut mid-thickness. The thickness of the shell elements is equal to the thicknesses of the bolt-head and nut, as shown in Fig. 4. The bolt shaft in actual bolts typically consists of two portions; (a) the bolt shank, i.e. the unthreaded part and (b) the threaded part. Both portions are represented with Hughes-Liu two-node beam elements (elform=1) with a diameter equal to the nominal diameter of the bolt. The junction between the beam elements of the bolt shaft and the shell elements of the bolt head is realized with constraint equations using the *CONSTRAINT_NODAL_RIGID_BODY (CNRB) keyword. The constraint nodes of the shell elements in the bolt-head and nut extend to an area that is equal to the area covered from the bolt shaft, as shown in Fig. 4(c). The CNRB definitions also include nodes at the ends of the beam elements to account for the actual deformable part of the bolt shaft as shown in Fig. 4(b). That is needed because the clear distance between the bolt head and nut, also known as grip length, is defined by the total thickness of the connecting parts and the thickness of the washers. The washers are modelled as separate parts that interact with the other components of the connection, i.e. bolt and connected plates. Fig. 5 shows the numerical model of the bolt/nut including the washers. The thinning option in the *CONTROL_SHELL card (istupd=4) was used since the elements at the vicinity of the bolt hole experience high plastic strains and Poisson’s ratio effect become influential.

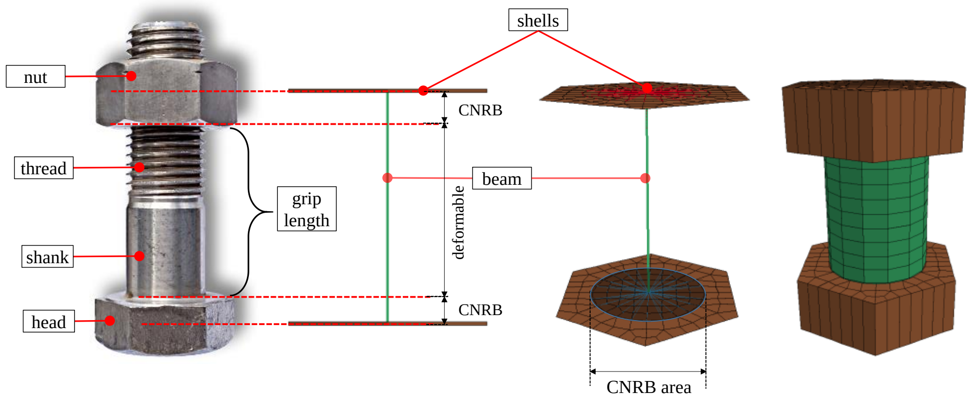

Fig. 4: Finite element model of bolt/nut, (a) actual bolt/nut, (b) plan view, (c) perspective view, (d) extruded view

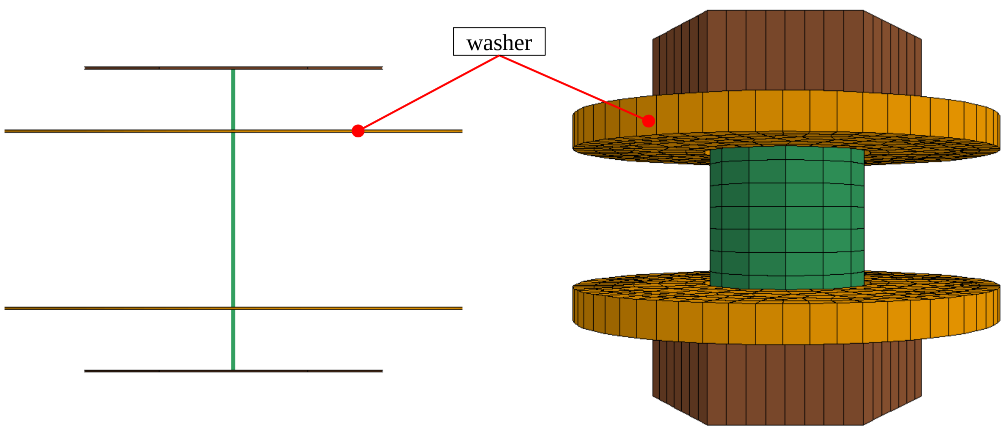

Fig. 5: Finite element model of the bolt/nut including washers, (a) plan view, (b) perspective view

The plates that are attached together with the bolts are represented with fully integrated shell elements. The bolt-hole should always be centered to the bolt-hole shaft to avoid any initial penetrations between them. The reference plane of the shell elements is always placed at the mid-thickness of the plates. Fig. 6 shows a side view of a complete single bolted connection finite element model including the plates. Around the bolt-holes of the plates, very thin null beam elements are used to account for the contact of the bolt shaft with the bolt-hole as shown in Fig. 7. The null beam elements do not have any structural contribution in the connection response and are implemented in LS-DYNA as regular beams that use the *MAT_NULL material definition. Null beams are also placed at the washers to account for the contact between the bolt shaft and the washers.

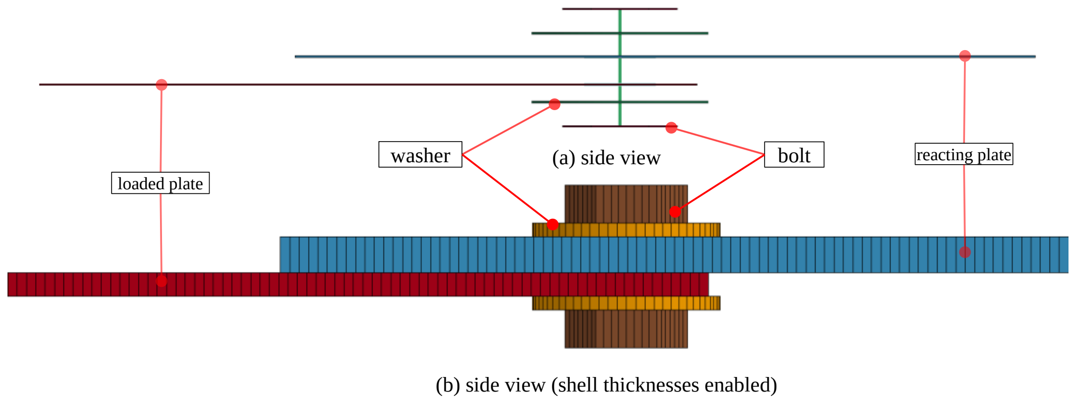

Fig. 6: Side view of the complete connection model

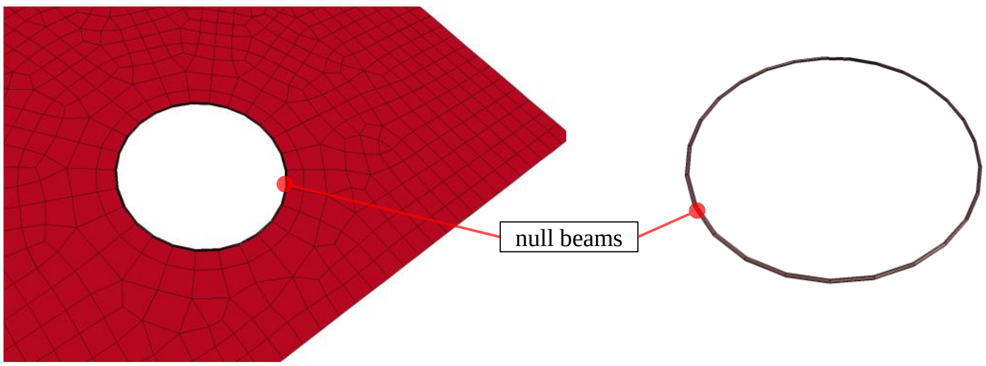

Fig. 7: A view of the plate depicting the null beam elements placed around the bolt-hole

Interaction of the Connecting Parts

The individual connection components interact with each other by defining two separate contact groups. The first group includes the beam elements of the bolt shaft and the null beam elements that are placed around the bolt-hole only. This contact group explicitly simulates the bearing stresses of the bolt shaft against the bolt hole using the *CONTACT_AUTOMATIC_GENERAL keyword. The second contact group includes the interaction of all remaining parts, i.e. the connected plates, bolt-head, nut, and washer using the *CONTACT_SINGLE_SURFACE keyword. In both contact definitions a static and dynamic friction coefficient of 0.5 and 0.4 are used respectively (fs=0.5, fd=0.4). Applying a viscous damping coefficient of 10-20% for the contact helps in eliminating high-frequency oscillations [4]. The contact option that ignores initial penetrations (IGNORE=2) is used because in cases where relatively thick and small elements are used, self-contact between the shell elements might result in early termination of the analysis without any meaningful results.

Bolt Pretension

Pretension in the bolt is applied using thermal contraction. The principle is to numerically shrink the bolt shaft by cooling it enough to result in the desired tension. That is an iterative process and usually a couple of iterations will result in finding the required temperature drop that results in the desired pretension in the bolt shaft. LS-DYNA does not currently have non-iterative preloading types for Hughes-Liu beam elements and therefore the only available option for bolt pretension is thermal contraction.

Material Constitutive Behavior

A number of material models in LS-DYNA can be used to simulate the behavior of the connection components. In this study the *MAT_SIMPLIFIED_JOHNSON_COOK was used to represent the steel plates and *MAT_PIECEWISE_LINEAR_PLASTICITY was used for the bolts. It is crucial to define the material law using actual experimental data as a benchmark for replicating physical uniaxial tension coupon tests with numerical tension coupons. The objective is to identify the correct true stress-strain parameters so that the resulting engineering stress-strain curve from the analysis is similar to the benchmark curve. This calibration process tends to be sensitive to the specific geometry and gage length and it is therefore suggested that numerical coupon geometries match those of the experimental tests.

Material Damage Criteria

An important aspect of the modeling procedure is the implementation of advanced damage models that are able to simulate the post-yield behavior of steel until rupture and capture behaviors associated in extreme loading conditions. In this study, damage is modelled using the GISSMO (Generalized Incremental Stress-State dependent damage Model) damage model. A detailed description of GISSMO is provided by Effelsberg *et al* [5]. In the analyses performed herein two different failure and two different mesh regularization criteria were employed.

The first failure criterion is triaxiality-dependent which associates the plastic strain at fracture of the shell elements with the level of triaxiality of each element. That is defined as a triaxiality curve (LCSDG) in GISSMO that associates the effective plastic strain at fracture for different triaxiality ratios. The dependence of fracture strain of steel with triaxiality has been proven by a number of researchers such as Johnson and Cook [8] but the experimental data available for different types of metals are still very limited.

The second failure criterion is the introduction of strain-rate dependent scaling factors for equivalent plastic strain to failure. A curve (LCSRS) defines scaling factors for the plastic strain at fracture at the different strain rates. This accounts for the fact that steel fractures at lower strains as the load rate increases. Data for these damage parameters were based on the experimental work of Whittington *et al.* [6].

The last two criteria basically implement mesh regularization for different mesh sizes. Those require the definition of two additional curves. The first one scales the equivalent plastic strain to failure with the element size (LCREGD). In general the scaling factors increase as the element sizes decreases. The second one defines a fading component that depends on the element size and accounts for the strain localization (FADEXP) at higher strain rates. Values for these two criteria were adopted from the work of Ozamut *et al*. [7] that focused on identification of these parameters for steel.

Remarks and Limitations of the Simplified Modeling Procedure

A number of parameters in the modeling procedure were found to have appreciable influence on the connection response. Those are discussed in this section and limitations associated with the simplified modeling procedure are also presented.

Bearing Forces

In an actual bolted connection or a detailed finite element model with brick elements, the bearing forces of the bolt shaft with the bolt holes are distributed over the contact area between the bolt shaft and the bolt holes, as shown in Fig. 8(a). Depending on the thickness of the connected plates and the diameter of the bolt, the contact area can increase significantly. On the other hand, when the proposed simplified connection model is used, this contact area is reduced to a contact edge, which consists of the shell elements around the bolt-hole that are in contact with the bolt shaft as shown in Fig. 8(b) and Fig. 9. Therefore the distribution of bearing forces due to that contact is different compared to the actual one and this results in a different stress distribution. This difference does not typically cause any issues at relatively low loads, but at higher loads, such that the connection is about to rupture, this can lead to significantly different results. A good approach that has been proven to provide better results is to always have the reference planes of the shell elements at their mid-thicknesses (nloc=0).

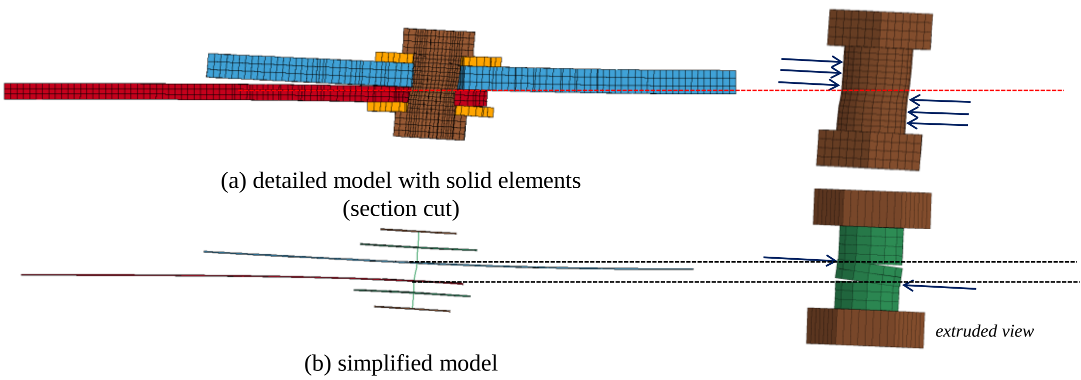

Fig. 8: Bearing forces, (a) detailed model with solid elements, (b) simplified model

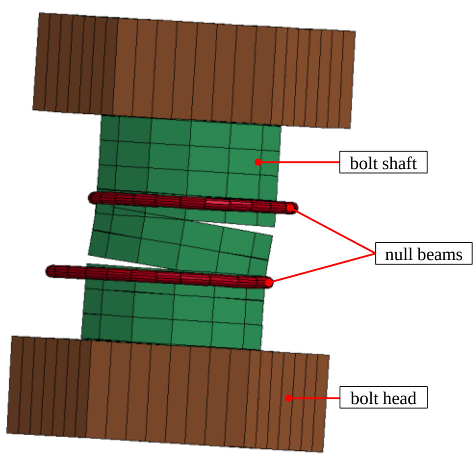

Fig. 9: Interaction of the bolt-shaft with the null beams in the simplified connection models

Triaxiality Damage Criterion

An important parameter is the definition of a triaxiality-dependent failure criterion, which affects the connection response, especially when plate tear-out fracture is modelled. Bearing of the bolt-shaft with the bolt-hole results in an uneven triaxiality state at the vicinity of the bolt-hole. An example of the triaxiality state of a plate that is bearing against a bolt is shown in Fig. 10(a). Fig. 10(b) shows the Von Misses stress distribution at the same state. It is noticeable that although the stresses at the bearing side of the bolt-hole are fairly uniform, the triaxiality ratios are considerably different. The definition of the fracture strain as a function of triaxiality ratio eventually dictates which of those elements fail first and results in a more realistic block shear failure as shown in Fig. 11(a). On the other hand, if the failure strain is independent of the triaxiality ratio, the failure mode is not realistic and is shown in Fig. 11(b). In that case elements fail right at the bearing surface between the bolt-shaft and the bolt-hole which also affects the obtained capacity of the connection.

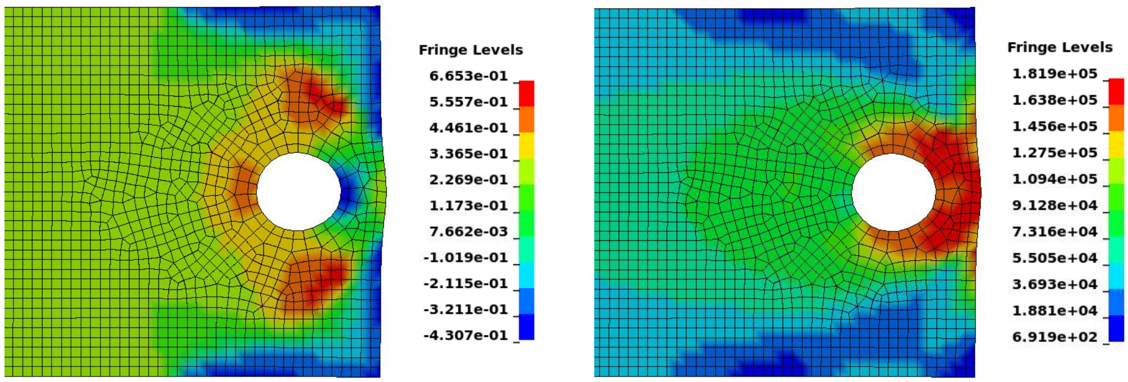

(a) Triaxiality ratio (b) Von-Misses stresses

Fig. 10: Triaxiality ratio and von-Mises contours on a plate that is bearing against a bolt (bolt not shown for clarity)

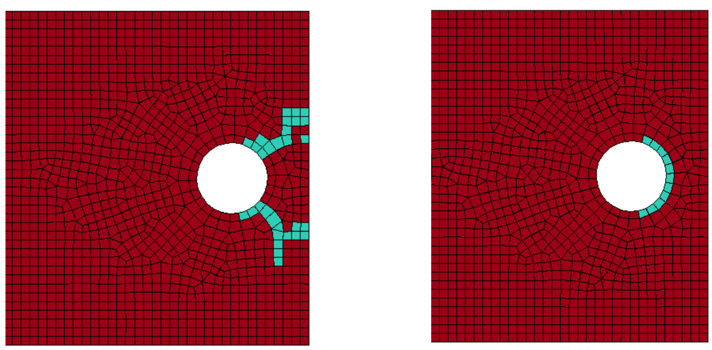

(a) triaxiality-dependent fracture (b) triaxiality-independent fracture

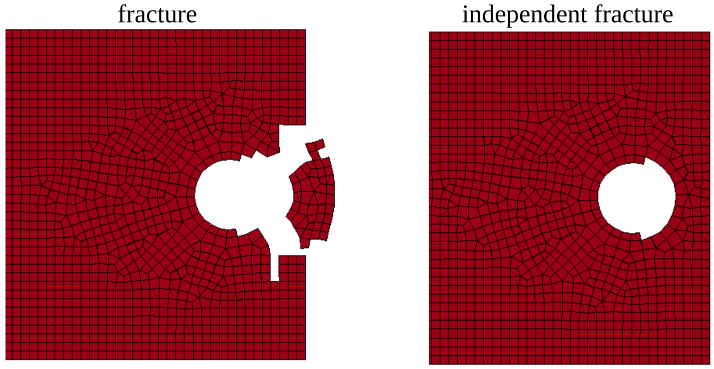

Fig. 11: Plate tear-out fracture, (a) triaxiality-dependent fracture, (b) triaxiality-independent fracture

Comparison with Experimental Tests

The static and dynamic pendulum tests of the connections were simulated to validate the proposed simplified modeling approach. For the dynamic tests a separate detailed finite element model of the pendulum testing was created as shown in Fig. 12. The connection specimens were represented with the simplified modeling approach presented herein and the remaining components of the test setup were included, such as the loading frame and the pendulum. For each test, the peak axial force that was developed at the specimen and the corresponding impact velocity of the pendulum were measured. Fig. 13 shows a comparison of the peak axial force versus the impact velocity of ten (10) of the dynamic pendulum tests against the response that was calculated with the finite element models. Each data series represents the same specimen configuration that was tested under different impact velocities. It is evident that these finite element models were able to capture the variation of the peak axial force under different impact velocities within 15%. Fig. 14 shows a comparison of the failure modes that were obtained with LS-DYNA and the failure modes of the physical tests. Both failure modes, i.e. plate tear-out fracture and bolt shear were quite similar to the failure modes that were observed during the physical tests.

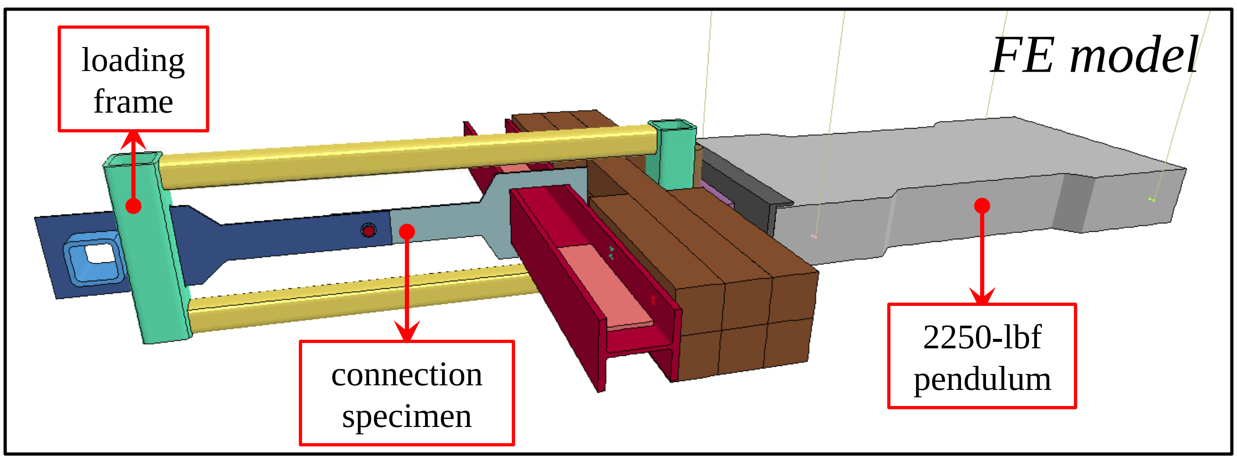

Fig. 12: Finite element model used to replicate the pendulum tests

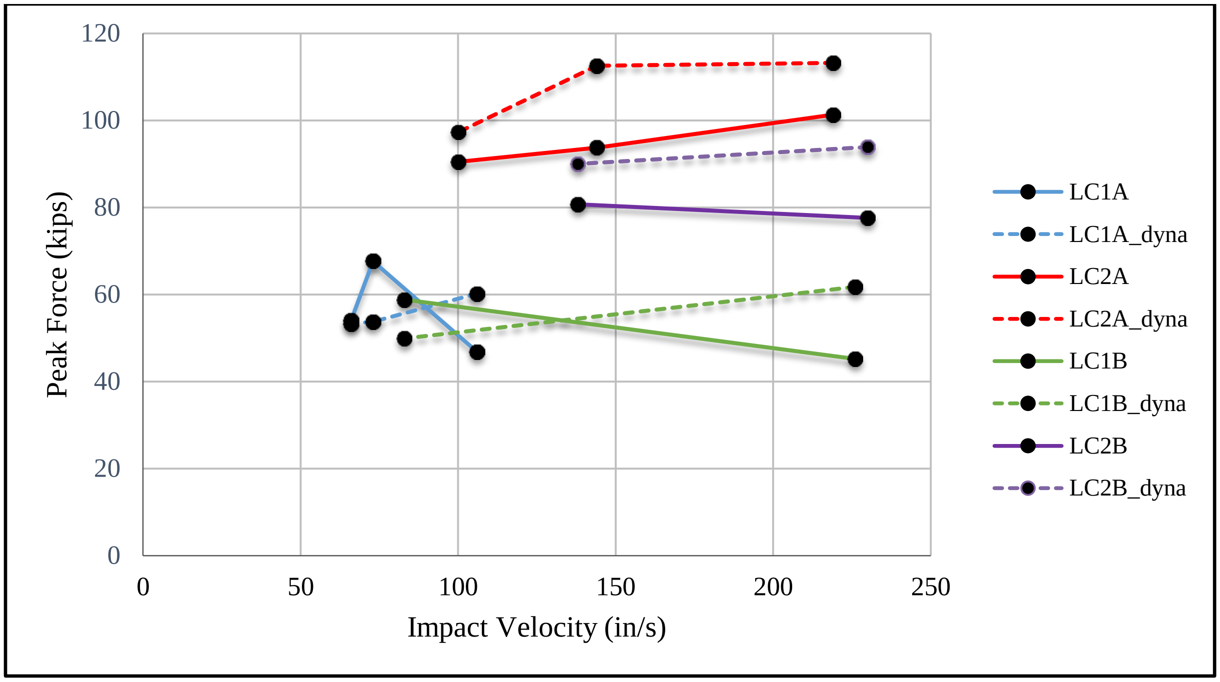

Fig. 13: Peak force versus impact velocity, experimental data and LS-DYNA simplified simulations

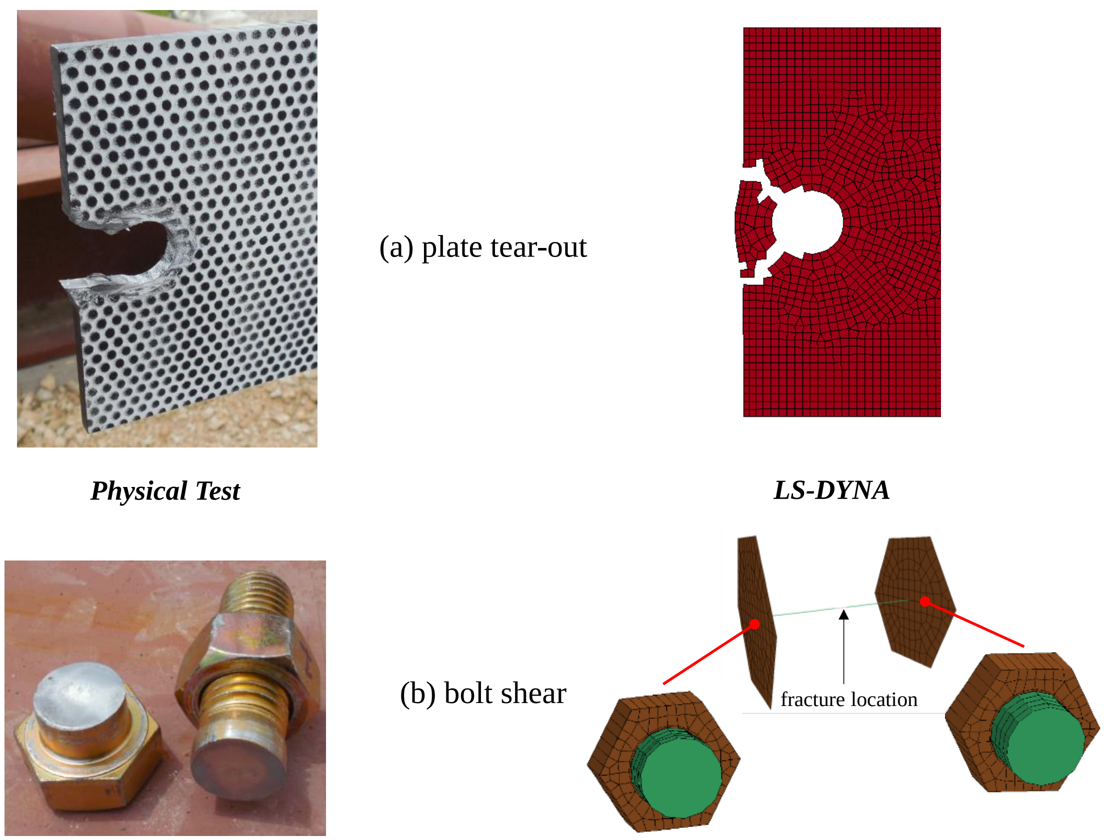

Fig. 14: Comparison of failure modes in the simplified bolted connection specimens modelled with LS-DYNA and the physical tests, (a) plate tear-out, (b) bolt shear

Summary

This paper presented a simplified modeling approach that can be used to model bolted connections under static and dynamic loading conditions. This approach can be used in large models with multiple connections and has been validated against static and dynamic test data. This methodology is proven capable of simulating the behavior of bolted connections until rupture with good accuracy. Crucial aspects of the modeling behavior for accurate simulation of the connection response and prediction of the failure modes associated with connection failure were discussed.

Acknowledgment

The authors would like to acknowledge Navistar Defense, LLC, for the contributions of materials used in testing and technical advice during the execution of this project.

References

[1] K.K. Nakalswamy, Experimental and numerical analysis of structures with bolted joints subjected to impact load, n.d.

[2] S. Narkhede, N. Lokhande, B. Gangani, G. Gadekar, Bolted joint representation in LS-DYNA to model bolt pre-stress and bolt failure characreristics in crash simulations, in: 2010.

[3] U. Sonnenschein, Modelling bolts under dynamic loads, in: 2008.

[4] Contact parameters — LS-DYNA Support, (n.d.). http://www.dynasupport.com/tutorial/contact-modeling-in-ls-dyna/contact-parameters (accessed September 18, 2015).

[5] J. Effelsberg, A. Haufe, M. Feucht, F. Neukamm, P. Du Bois, On parameter identification for the GISSMO damage model, in: Dearborn, MI, USA, n.d.

[6] W.R. Whittington, A.L. Oppedal, S. Turnage, Y. Hammi, H. Rhee, P.G. Allison, et al., Capturing the effect of temperature, strain rate, and stress state on the plasticity and fracture of rolled homogeneous armor (RHA) steel, Mater. Sci. Eng. A. 594 (2014) 82–88. doi:10.1016/j.msea.2013.11.018.

[7] B. Ozarmut, H. Richter, A. Brosius, Parameter identification of a damage model for the process chain “forming crash,” in: 2014.

[8] G.R. Johnson, W.H. Cook, Fracture characteristics of three metals subjected to various strains, strain rates, temperatures and pressures, Eng. Fract. Mech. 21 (1985) 31–48. doi:10.1016/0013-7944(85)90052-9.